This is an open access article published under a Creative Commons Attribution (CC-BY) License, which permits unrestricted use, distribution and reproduction in any medium, provided the author and source are cited.

ACS APPLIED MATERIALS & INTERFACES

Research Article

www.acsami.org

Ultraefficient Cap-Exchange Protocol To Compact Biofunctional Quantum Dots for Sensitive Ratiometric Biosensing and Cell Imaging

Weili Wang,[†] Yuan Guo,[†] Christian Tiede,[‡] Siyuan Chen,[§] Michal Kopytynski,[§] Yifei Kong,[†] Alexander Kulak,[†] Darren Tomlinson,[‡] Rongjun Chen,[§] Michael McPherson,[‡] and Dejian Zhou*[,†]

[†]School of Chemistry and Astbury Structure for Molecular Biology and [‡]School of Molecular and Cellular Biology and Astbury Structure for Molecular Biology, University of Leeds, Leeds LS2 9JT, United Kingdom

[§]Department of Chemical Engineering, Imperial College London, South Kensington Campus, London SW7 2AZ, United Kingdom

Supporting Information

ABSTRACT: An ultraefficient cap-exchange protocol (UCEP) that can convert hydrophobic quantum dots (QDs) into stable, biocompatible, and aggregation-free water-dispersed ones at a ligand:QD molar ratio (LQMR) as low as 500, some 20−200-fold less than most literature methods, has been developed. The UCEP works conveniently with air-stable lipoic acid (LA)-based ligands by exploiting tris(2-carboxylethyl phosphine)-based rapid in situ reduction. The resulting QDs are compact (hydrodynamic radius, R_h, < 4.5 nm) and bright (retaining > 90% of original fluorescence), resist nonspecific adsorption of proteins, and display good stability in biological buffers even with high salt content (e.g., 2 M NaCl). These advantageous properties make them well suited for cellular imaging and ratiometric biosensing applications. The QDs prepared by UCEP using dihydrolipoic acid (DHLA)-zwitterion ligand can be readily conjugated with octa-histidine (His_8)-tagged antibody mimetic proteins (known as Affimers). These QDs allow rapid, ratiometric detection of the Affimer target protein down to 10 pM via a QD-sensitized Förster resonance energy transfer (FRET) readout signal. Moreover, compact biotinylated QDs can be readily prepared by UCEP in a facile, one-step process. The resulting QDs have been further employed for ratiometric detection of protein, exemplified by neutravidin, down to 5 pM, as well as for fluorescence imaging of target cancer cells.

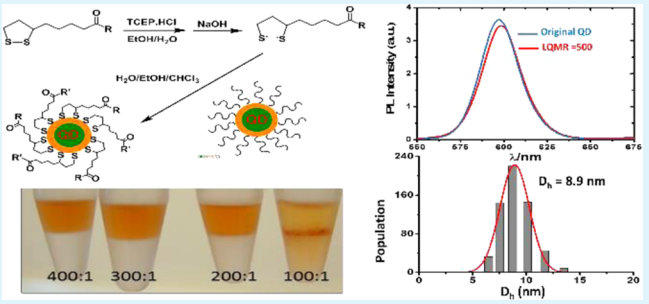

KEYWORDS: *quantum dot, cap exchange, ultraefficiency, Förster resonance energy transfer, fluorescence, ratiometric sensing, cell imaging*

INTRODUCTION

Over the past two decades, quantum dots (QDs) have been of significant research focus due to their unique, size-dependent, stable, and bright fluorescence, thus making them powerful probes for a wide range of applications such as energy, materials, biology, and medicine.[1−11] Their broad absorption and stable, narrow symmetric emission are particularly well suited for multiplexed sensing, biodiagnostics, bioimaging, immunoassay, cell tracking, and trafficking studies.[3−6,9,12−20] In this regard, a robust, compact, and biocompatible QD structure is of paramount importance. However, since most high-quality QDs (e.g., CdSe/ZnS, CdSe/CdS/ZnS, CdSe/ZnSe/ZnS) are prepared by an organometallic route, they are naturally capped with hydrophobic ligands which render them nondispersible in aqueous solution and biologically incompatible.[3,4,16] To produce biocompatible QDs, three main approaches are widely employed: (1) encapsulation with PEGylated phospholipids or amphiphilic/block copolymers,[4,16,21] (2) coating with silica,[3] and (3) cap exchange.[4,6] The first two methods can produce stable but relatively bulky QDs with a typical hydrodynamic radius (R_h) of >10 nm. This large size can limit their application in bioimaging, particularly in crowded regions such as neuronal synapses[22] and more critically in Förster resonance energy transfer (FRET)-based applications. This is because such R_hs are already greater than the R_0 (Förster radius) values of most QD−dye FRET pairs (i.e., 4−7 nm) prior to bioconjugation.[9] Given the inverse sixth power dependence of FRET efficiency (E) on the donor−acceptor distance (r), $E = 1/[1 + (r/R_0)^6]$, such bulky QDs will lead to diminished E and hence low sensitivity.[3,19,23,24] By contrast, cap exchange can produce compact QDs which are better suited to FRET-based applications.[12−14,17−19,25−32] Optimizing the cap-exchange process with 3-mercaptopropionic acid has allowed the QD to retain high fluorescence.[31] However, such monodentate ligand-capped QDs often display limited stability and/or resistance to nonspecific adsorption,[25,32] especially in biological media with high salt content. By contrast, dihydrolipoic acid (DHLA)-,[28,29,33−36] bis-

Received: October 28, 2016
Accepted: April 19, 2017
Published: April 19, 2017

 © 2017 American Chemical Society

DOI: 10.1021/acsami.6b13807
ACS Appl. Mater. Interfaces 2017, 9, 15232−15244

Table 1. Comparison of Cap-Exchange Conditions and Retained Fluorescence for Some DHLA-Based Ligand-Capped QDs[a]

LQMR (in 10^3)	time	QD type	ligand	retained original QD fluorescence (%)	ref
~42	~2 h	CdSe/$Zn_xCd_{1-x}S$	DHLA-PEG-NH_2	46−62	34
~22	~0.5 h	CdSe/ZnS	DHLA-SB	29−43	35
~22	~0.5 h	CdSe/CdS/ZnS	DHLA-SB	71−85%	35
~40	60 min ($h\nu$)	CdSe/ZnS	Bis(LA)-ZW	50−70	37
~41	2 h	CdSe/ZnS	DHLA-Zn^{2+}	28−57	44
~22−50	~20 min ($h\nu$)	CdSe/ZnS	LA-PEG/NH_2/F	50−70	47
40−60	~30 min ($h\nu$)	CdSe/ZnS	LA-PEG/F	50−70	49
10−100	2 h	InP/ZnS	DHLA	11	50
~10	~2 h	CdSe/ZnS	DHLA	3.4−53[b]	51
~40	2.5 h	CdSe/CdS	DHLA-PEG	~8	52
~40	2.5 h	CdSe/CdS/ZnS	DHLA-PEG	~26	52
98	overnight	CdSe/ZnS	DHLA-F	40−57%	53
0.5	~1 min	CdSe/ZnS	DHLA-PEG/ZW	>90	this work
0.6	~1 min	CdSe/ZnSe/ZnS	DHLA-ZW	>95	this work

[a] $h\nu$: photoirradiation. DHLA-F: DHLA modified with functional group. [b] The retained QD fluorescence varied significantly for different colored QDs.

DHLA-,[37,38] and multidentate polymer-based ligands[39−41] can bind in a multivalent manner to the QD surface to provide a more robust coating. Moreover, such coating can also resist nonspecific adsorption upon incorporating a poly(ethylene glycol) (PEG) or zwitterion terminal group. The resulting compact, biocompatible QDs have been demonstrated to be powerful probes with a broad range of biomedical applications.[22,33−35,39−41]

Despite significant research, two limitations still remain to be solved for most current cap-exchange methods: (1) the requirement for a large excess of ligand (with ligand:QD molar ratio, LQMR, of ca. 10^4−10^5, Table 1) which limits its use with precious or expensive ligands and (2) a sizable reduction of fluorescence over the parent hydrophobic QDs (by ca. 15−95%, depending on the QD types and cap-exchange procedure) which compromises their fluorescence applications. Most current cap-exchange reactions are performed in two immiscible phases using non- or partially deprotonated ligands which are not optimal for rapid QD−ligand transport, exchange, or strong binding. Theoretically, a spherical 4.5 nm diameter red-emitting ($\lambda_{EM} \approx 600$ nm) CdSe/ZnS QD (see Supporting Information, SI, Figure S1A) has a total surface area of 63.6 nm^2. Assuming the QD is terminated with a full Zn^{2+} outer layer in stable Wurtzite structure with each Zn^{2+} occupying a surface area of 0.126 nm^2 (SI, Figure S2) then the QD would contain 505 surface Zn^{2+} ions. Assuming each thiolate binds to one Zn^{2+} ion, then 505 single thiolate ligands (or 253 DHLA-based ligands which contains 2 thiol groups each and hence a footprint of 0.252 nm^2) would completely saturate the QD surface Zn^{2+} ions. Note this is the theoretical maximum number; the actual number is likely to be lower because the QD surface may not be fully terminated with Zn^{2+} ions. Consistent with this proposal, the Mattoussi group recently reported a footprint of ~0.5 nm^2 for each LA-PEG1000-benzaldehyde ligand on a CdSe/ZnS QD surface, about twice that of our estimate. The slightly bigger footprint value is reasonable considering the possible steric effect of the long PEG chain as well as the nonpure zinc layer nature of the QD surface.[42] This simple calculation reveals that only a tiny fraction (ca. ≤ 2%) of the DHLA-ligands used in current literature methods can actually bind to the QD, with the vast majority remaining as free ligands. Given its strong Zn^{2+} binding affinity, such free DHLA-ligands may etch the ZnS protecting shell, generating surface defects (e.g., Zn^{2+}/S^{2-} vacant sites as hole/electron traps respectively via electrostatic attraction) and compromising the QD fluorescence.[28] Consistent with this suggestion, the Hollingsworth group found that treating an amphiphilic polymer-encapsulated QD with moderate concentrations of deprotonated 2-mercaptoethanol (MBE) reduced the QD surface electron trap (presumably by thiolates occupying the S^{2-} vacant sites) but produced new hole traps at higher concentrations (presumably by generating new Zn^{2+} vacant sites on the ZnS shell via etching).[43] Moreover, we previously found that treating a DHLA-based chelating dendritic ligand-capped CdSe/ZnS QD with either S^{2-} or Zn^{2+} ions could significantly enhance the QD fluorescence (~3 fold), presumably by passivating the surface electron/hole traps.[28] This conclusion is further supported by a recent report that cap exchange using Zn^{2+}-metalated DHLA better preserved QD fluorescence than free DHLA, presumably because the introduced Zn^{2+} ions minimized the ZnS shell etching.[44]

On the basis of this experimental evidence, we hypothesize that reducing the number of ligands to a level just sufficient for capping the QD surface Zn^{2+} ions should minimize any possible ZnS shell etching (Zn^{2+}/S^{2-} vacant site formation), allowing the cap-exchanged QD to retain native fluorescence. To achieve this goal, it is vital to improve cap-exchange efficiency. We recently demonstrated substantial improvement of efficiency by performing a cap-exchange reaction in a homogeneous solution using deprotonated DHLA-ligands,[45] due to the greatly improved QD−ligand transport/exchange rates and enhanced binding affinity. Despite this success, it remained a laborious and delicate process because the DHLA-based ligands had to be freshly prepared, purified by column chromatography, and used in the same day to ensure a successful cap exchange. This is because the DHLA-based ligands are air sensitive and susceptible to oxidization to their LA forms, which results in loss of QD binding affinity.[46] By contrast, the photoligation method developed by the Mattoussi group can work directly with the air-stable LA form of ligands.[46−49] However, the requirement for a large excess of ligands (LQMR = 2−4 × 10^4, Table 1) can limit its application with precious or expensive ligands. Thus, an efficient cap-exchange method that uses the minimum amount (ca. LQMR < 1000) of air-stable ligands without lengthy separation and/or purification steps and

DOI: 10.1021/acsami.6b13807
ACS Appl. Mater. Interfaces 2017, 9, 15232−15244

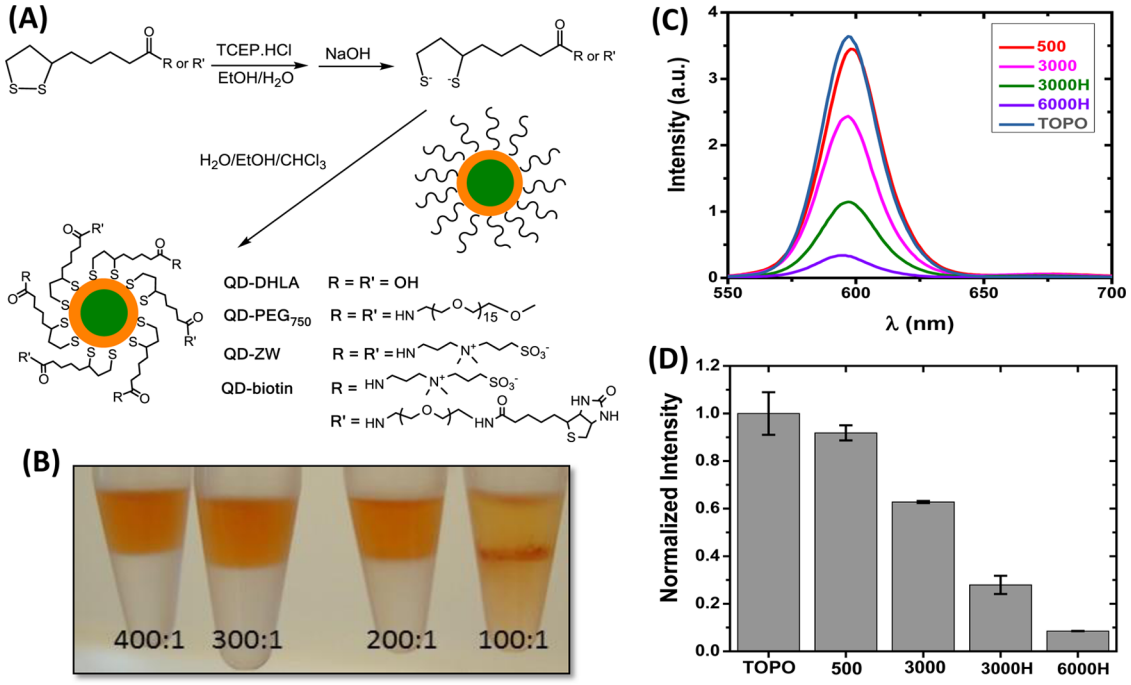

Figure 1. (A) Schematic procedures of our UCEP to compact, biocompatible QDs capped with DHLA-based ligands. (B) Photograph of a CdSe/ZnS QD ($\lambda_{EM} \approx 600$ nm) after cap exchange with DHLA-ZW under LQMRs: (top layer) water, (bottom layer) $CHCl_3$. (C) Fluorescence spectra of a CdSe/ZnS QD prior to (10 nM in $CHCl_3$, TOPO) and after cap exchange with DHLA-ZW (10 nM in H_2O) under different LQMRs without and with heating (the LQMR is indicated for each sample; **H** stands for heating at 70 °C for 1 h). (D) Comparison of the relative fluorescence intensity of the above QDs (data shown as mean ± standard deviation, $n = 3$).

compromising the cap-exchanged QD fluorescence would be extremely valuable for QD biomedical applications.

Herein, we report an ultraefficient cap-exchange protocol (UCEP) that satisfies such requirements. It is based on a rapid reduction of LA-based ligands to their DHLA forms by tris(2-carboxylethyl)phosphine (TCEP). After deprotonation of the thiol groups, the in situ reduced DHLA-based ligands are directly used to initiate cap exchange with the hydrophobic CdSe/ZnS or CdSe/ZnSe/ZnS QDs in a homogeneous solution. We show that UCEP can completely transform the hydrophobic QDs into stable, aggregation-free water dispersions at a LQMR as low as 500, ~20−200-fold lower than most current literature protocols (Table 1). Moreover, the resulting QDs are compact ($R_h < 4.5$ nm), retain > 90% of their original fluorescence, and resist nonspecific adsorption, making them powerful fluorescence probes for FRET-based ratiometric sensing and cancer cell imaging.

RESULTS AND DISCUSSION

Our UCEP procedure is shown schematically in Figure 1A. First, three LA-based ligands appending different terminal functional groups (e.g., PEG750, zwitterion, PEG600-biotin; see Chart 1 for chemical structures) were synthesized by following literature reported procedures.[29,45,48] The ligands were then purified by silica gel column chromatography (for LA-PEG750 and LA-PEG600-biotin) or high-performance liquid chromatography (HPLC, for LA-zwitterion). Details of the synthetic procedures and spectroscopic data to confirm ligand purity and chemical identity are given in the SI.

Next, the LA−ligand (e.g., LA-ZW) was reduced quantitatively to its DHLA form by 1 mol equiv of TCEP·HCl in a mixed solvent of ethanol/water (1:1 v/v). The reduction was complete in ~5 min and could be directly visualized by the

Chart 1. Chemical Structures of the Lipoic Acid (LA)-Based Ligands Used in This Study

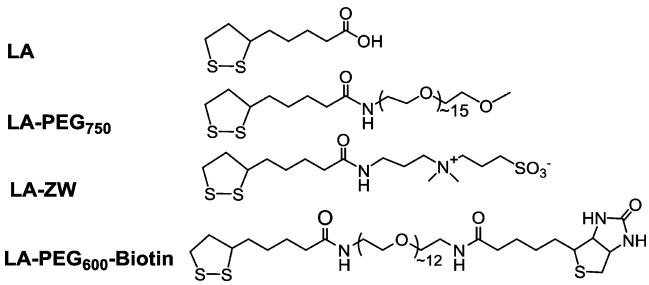

disappearance of the yellow color (originating from the dithiolane ring absorption), yielding a clear colorless solution. Then six DHLA-ligand molar equivalents of NaOH (in ethanol) were added to deprotonate the DHLA dithiol groups to enhance their QD binding affinity.[44] Six molar equivalents of NaOH were used because each DHLA-based ligand contains two thiol groups and each TCEP.HCl molecule contains 4 acid groups. The in situ reduced ligand was then added directly into a QD sample dissolved in a mixed solution of $CHCl_3$ and ethanol (5:2 v/v), forming a homogeneous solution. After brief shaking, the QDs were found to rapidly rise (<1 min) to the upper aqueous layer (note, the mixed $CHCl_3$/EtOH/H_2O solution itself did not phase separate in the absence of the QD and/or ligands), indicating the formation of hydrophilic QDs. The phase separation became clearer after adding more water followed by a brief centrifugation (20 000 × g for 60s), where all QDs were found in the top aqueous layer, leaving the lower $CHCl_3$ layer colorless (Figure 1B), indicating full QD water phase transfer. The aqueous layer was then transferred to a centrifugal filtration tube with a 30 000 MW cutoff membrane.

DOI: 10.1021/acsami.6b13807
ACS Appl. Mater. Interfaces 2017, 9, 15232−15244

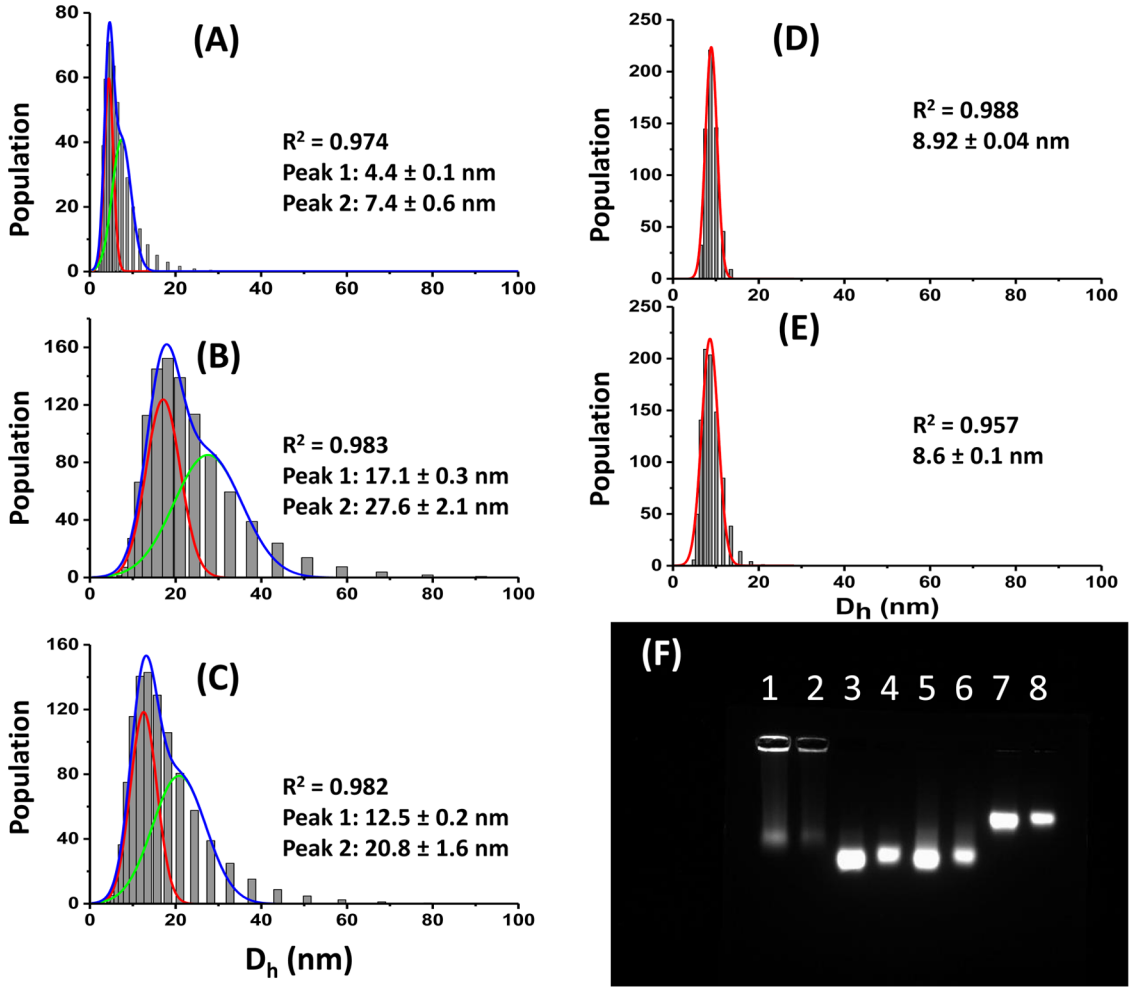

Figure 2. Hydrodynamic diameter (volume population, $D_h = 2R_h$) distribution histograms of a CdSe/ZnS core/shell QD ($\lambda_{EM} \approx 600$ nm) before (A, in hexane) and after cap exchange with DHLA-ZW at different LQMRs: 200 (B); 300 (C); 500 (D); 1000 (E). Fitting the histograms by Gaussian function revealed that A–C contained two different size species while D and E contained just one species. (F) Gel electrophoresis diagram of the CdSe/ZnS QD after cap exchange with DHLA-ZW at a LQMR of 200 (lanes 1 and 2), 500 (lanes 3 and 4), 1000 (lanes 5 and 6), and 500 mixed with a His_8-tagged Affimer at a protein:QD molar ratio of 10:1 (lanes 7 and 8). Sample volumes were 5 μL for lanes 1, 3, 5, and 7 and 2 μL for lanes 2, 4, 6, and 8.

After three rounds of centrifugation and washing with H_2O to remove unbound free ligands, a stable well-dispersed QD stock aqueous solution was obtained.

UCEP with CdSe/ZnS Core/Shell QD. First, we investigated how LQMR affected the cap-exchange process using the most widely used commercial hydrophobic CdSe/ZnS core/shell QD capped with the mixed trioctylphoshine/trioctylphoshine oxide ligands ($\lambda_{EM} \approx 600$ nm, ~4.5 nm core diameter, Figure S1) and the DHLA-zwitterion (ZW) ligand (Chart 1).

When the cap exchange was performed at a LQMR of ≥200, all of the CdSe/ZnS QDs were fully transferred to the upper aqueous phase (shown as a brownish color), leaving the lower $CHCl_3$ layer colorless. By contrast, the $CHCl_3$ layer still contained some untransferred QDs at a LQMR of 100, indicating that 200 is the minimum ratio required for complete QD water dispersion (Figure 1B). Deprotonation of the DHLA thiol groups was essential for a successful cap exchange. The use of the TCEP-reduced DHLA-ZW ligand directly without thiol group deprotonation produced no observable QD phase transfer at 200 LQMR: all the QDs were found to remain in the organic phase. This result agrees well with earlier reports that thiolates bind much more strongly to Zn^{2+} ions than do free thiols.[31,44] The use of NaOH deprotonated TCEP only in the absence of DHLA-ZW ligand also produced no observable QD phase transfer, suggesting that TCEP or oxidized TCEP was not the driving force behind the rapid, efficient QD phase transfer observed here.

We subsequently investigated how LQMR affected the fluorescence of the UCEP-prepared QDs. When cap exchange was performed at LQMRs of ≤500 (i.e., ≤ the total number of the estimated Zn^{2+} ions on the QD surface), all of the cap-exchanged QDs effectively retained the native fluorescence of the parent hydrophobic QD in $CHCl_3$ (>90%, Figure 1 and Figure S3). The level of retained fluorescence here is considerably higher than most other reports for the CdSe/ZnS QDs (Table 1). The retained fluorescence was reduced to ~67% as LQMR was increased to 3000 (Figure 1C). This observation that increasing the LQMR results in a lower retained QD fluorescence agrees well with our hypothesis that excess free ligands are indeed responsible for quenching fluorescence of the cap-exchanged QD, possibly by etching its ZnS shell. This mechanism was verified by analyzing the total Zn^{2+} and Cd^{2+} contents of the CdSe/ZnS QD after cap

DOI: 10.1021/acsami.6b13807
ACS Appl. Mater. Interfaces 2017, 9, 15232–15244

exchange with DHLA-ZW at different LQMRs by atomic absorption spectroscopy: a small but measurable decrease of the Zn^{2+}/Cd^{2+} molar ratio of ca. 3.5% (from 1.96 ± 0.01 to 1.89 ± 0.02) was observed as the LQMR was increased from 500 to 10 000 (see SI, section D7, Figure S4). Heating was also found to impact on the retained QD fluorescence. For example, at a LQMR of 3000, heating at ~70 °C for 1 h produced a QD displaying one-half the intensity of its nonheated counterpart (Figure 1D). Further increasing the LQMR to 6000 with 1 h heating using our previously reported cap-exchange procedures[29,30] yielded an even more severely quenched QD, retaining just ~10% of the original fluorescence. These results indicate that heating is likely to accelerate the ZnS shell etching by free DHLA-ZW ligands.

The DHLA-ZW-capped CdSe/ZnS QD (abbreviated as QD−ZW) prepared by UCEP was stable in phosphate buffer saline (PBS, 10 mM phosphate, 150 mM NaCl, pH 7.4) over a pH range of 6−10 and even with high salt conditions (e.g., 2 M NaCl, Figure S5). The stability of our QD was broadly in line with other DHLA−zwitterion ligand-capped QDs.[47,48] Importantly, the UCEP was a rapid process. Complete transfer of the QD into the aqueous phase was observed in <1 min, which was much faster (ca. 20−200-fold) than most literature methods using two immiscible phases (Table 1). This greatly improved performance was attributed to the greatly enhanced QD−ligand exchange and transfer rates in homogeneous solution as well as greatly enhanced affinity between the QD and the DHLA-ZW ligands after thiol deprotonation. Interestingly, despite not being the driving force behind the rapid QD water-phase transfer, the presence of oxidized TCEP during the cap-exchange process did improve the retained QD fluorescence: while >90% of original fluorescence was retained for the UCEP-prepared QD in the presence of oxidized TCEP at 500 LQMR with the DHLA-ZW ligand (Figure 1), this number was decreased to ~80% for a control QD under equivalent conditions but without oxidized TCEP (Figure S6). This result was fully consistent with a previous report by the Reiss group with an InP/ZnS QD and other thiolated ligands.[50] It is likely that, at low LQMRs, a small number of oxidized TCEP molecules may bind to the QD surface to partially passivate the hole traps to improve the QD fluorescence while also aiding the QD water-phase transfer from its hydrophilic nature. At high LQMRs, ZnS shell etching by the large excess of DHLA-based ligands becomes dominant, leading to severe quenching of the QD fluorescence. Hence, the oxidized TCEP may play two beneficial roles: improving the retained fluorescence and aiding QD phase transfer; both factors contribute to the ultraefficiency of the UCEP.

The UCEP was readily applied to other DHLA-based ligands such as DHLA-PEG750, where a LQMR of 200 was also sufficient to completely water disperse the CdSe/ZnS QD (SI, Figure S3). Again, the cap-exchanged QDs retained >90% of their original fluorescence and were stable for >1 week. Such a gentle yet robust approach is particularly well suited for core/shell QDs with relatively thin ZnS shells (which is the case for most commercially available CdSe/ZnS QDs) whose fluorescence is highly sensitive to changes of environmental conditions (e.g., oxidation, precipitation, etc.) and can be badly affected following cap exchange with strongly coordinating ligands.[28,54] This is likely due to the ZnS shell being too thin to completely confine the exciton carriers within the core despite its type I core/shell QD structure. The exciton carriers can "leak" out of the thin shell (via residual wave functions that can extend ~0.8 nm into the shell from the simulations reported by the Bawendi group)[55] and get trapped by surface defects (e.g., S^{2-}/Zn^{2+} vacant sites) induced by cap exchange with such strongly coordinating ligands.

The hydrodynamic radius (R_h, which equals $1/2D_h$) of a QD is critical for its biomedical applications.[9,22] Hence, the R_h values of the CdSe/ZnS QD after cap exchange with the DHLA-ZW ligand under different LQMRs were investigated by dynamic light scattering (DLS, see Figure 2).[45] Interestingly, the water-dispersed QDs prepared at LQMRs of 500 and 1000 were compact (R_h < 4.5 nm) and displayed almost identical, uniform narrow size distributions. This R_h value was comparable to those of other well-dispersed small-molecule ligand-capped QDs reported in the literature,[35,45,50] suggesting that these QDs formed isolated, aggregation-free water dispersions. However, the QDs prepared at LQMRs of 200 and 300 displayed relatively large, dual-size distributions. Using the parameters obtained from the Gaussian fits, their average R_hs were calculated as ~11.5 and ~8.5 nm, respectively. The corresponding particle volumes were ~20 or ~8 times those of individual QDs, suggesting the QDs prepared at 200 or 300 LQMR formed minor aggregates or clusters (see SI, Table S1). These results suggest that a LQMR of 200 or 300 is too low to completely displace the original ligands on the QD surface. As a result, the residual hydrophobic ligands that remained on the QD surface can lead to QD aggregation/clustering via hydrophobic interactions.

The different QD sizes were further verified by gel electrophoresis analysis:[45] the QD prepared at 200 LQMR apparently showed evidence of aggregation and exhibited lower gel mobility (larger sizes) than those prepared at 500 or 1000, where the latter two displayed identical gel mobility (Figure 2F). Nevertheless, the gel mobility results are fully consistent with the R_h measurements by DLS. Together, these results indicate that not all of the added DHLA-ligands may have bound to the QD or the dithiolates in each DHLA molecule may chelate to one Zn^{2+} ion rather than bind to two separate Zn^{2+} ions on the QD surface. Therefore, a DHLA-ligand:QD surface Zn^{2+} molar ratio of ~1:1 (rather than the original estimate of 1:2) is required to produce compact, aggregation-free QDs suitable for practical biomedical applications.

UCEP with CdSe/ZnSe/ZnS QD. Besides the CdSe/ZnS core/shell QD, the UCEP was readily extended to different colored CdSe/ZnSe/ZnS core/shell/shell QDs with λ_{EM}s = 525, 575, and 606 nm (Figure S1B). The core/shell/shell QDs have robust fluorescence because their CdSe fluorescent cores are protected by two layers of thicker inorganic shells. This is supported by evidence from the literature showing significantly higher fluorescence was typically retained for the core/shell/shell QDs over their core/shell (CdSe/ZnS) counterpart after cap exchange with DHLA-based ligands under equivalent conditions (Table 1).[35,52] All three different colored CdSe/ZnSe/ZnS QDs were fully water dispersed after cap exchange with the DHLA-ZW ligand at a LQMR of 200. Moreover, these water-dispersed QDs also retained >95% of their original fluorescence (see SI, Figure S7). It was noticed, however, that while a LQMR of 200 led to water dispersion, the resulting QDs lacked long-term stability and eventually precipitated from the aqueous solution within 1 week. Increasing the LQMR to 600 produced highly stable, biocompatible QDs that remained visibly clear without any noticeable changes of physical appearance or fluorescence over >3 months. The UCEP-prepared water-dispersed QDs also retained >95% of their

DOI: 10.1021/acsami.6b13807
ACS Appl. Mater. Interfaces 2017, 9, 15232−15244

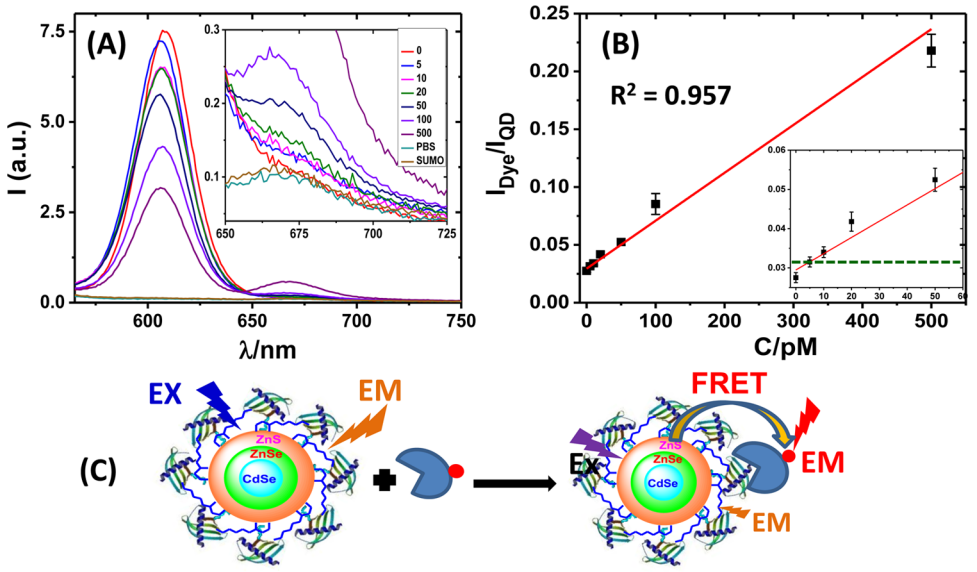

Figure 3. (A) Fluorescence spectra of the QD−Affimer (final C_{QD} = 0.50 nM) after incubation with different concentration of the target SUMO protein (Alexa-647 labeled) in PBS containing 1 mg/mL of bovine serum albumin. Inset shows the amplified FRET signals over 650−725 nm. Note that the backgrounds of PBS and PBS+10 nM labeled SUMO protein are almost the same. (B) Plot of the integrated fluorescence intensity ratio (I_{Dye}/I_{QD}) between the dye (over 650−750 nm) and the QD (over 560−650 nm) versus the SUMO protein concentration fitted to a linear function. Inset shows the response over 0−50 pM, and the green dashed line indicates the limit of detection (background + 3σ). (C) Schematic presentation of the QD−Affimer for detection of labeled target SUMO via QD-sensitized Alexa-647 FRET readout strategy.

original fluorescence. These findings contrast with most literature methods which report >50% fluorescence reduction even for such photochemically robust CdSe/CdS/ZnS core/shell/shell[52] or CdSe/Zn*x*Cd1-*x*S alloyed shell[34] QDs after cap exchange with DHLA-based ligands (Table 1). The exception is one example where up to 86% of original fluorescence was retained for a CdSe/CdS/ZnS QD.[35] These results demonstrate the general applicability of this UCEP approach and its excellent ability of retaining high fluorescence for cap-exchanged QDs.

QD−Affimer for Ratiometric Biosensing. The high fluorescence, compact structure, and robust stability in biologically relevant buffer of the UCEP-prepared QDs make them extremely attractive for FRET-based applications. This is because a compact QD gives a small r value while the high QD fluorescence yields a large R_0 value, both factors are strongly beneficial to improve E and hence sensitivity ($E = 1/[1 + (r/R_0)^6]$). Since r is not only determined by the QD but also the biorecognition molecule (binder), the use of small binders is also critical to improve E as reported by the Hildebrandt group.[56,57] Here, nonantibody binding proteins (known as Affimers, and first reported as Adhirons) were employed as binders for target proteins.[58] Compared to the widely used antibodies, Affimers have advantages of high thermal stability (typically $T_m \geq 80$ °C), similar binding affinities (nM K_d), high specificity, high yield animal-free recombinant bacterial production, and ease of incorporating site-specific functional tags (e.g., His_8, cysteine) for oriented bioconjugation to maximize binding site accessibility.[58−60] More importantly, their small sizes (MW ≈ 12 kDa, <10% that of a whole antibody) are especially attractive for FRET-based applications, allowing for significantly reduced r and thereby improved sensitivity. To demonstrate this potential, an Affimer that specifically recognizes the yeast small ubiquitin-like modifier (SUMO) protein was employed as a proof of concept for detecting target SUMO protein. SUMO proteins play an important role in a number of cellular process which include nuclear-cytosolic transport, transcriptional regulation, apoptosis, protein stability, and response to stress, making them useful diagnostic markers for genotoxic stress, cancer development, and proliferation.[58]

First, we studied the QD−Affimer conjugation via a highly efficient His_8-tag-metal affinity self-assembly.[5,61] The C-terminal His_8-tagged Affimer was reacted with an Alexa-647-NHS ester dye, yielding an average labeling of 1.06 Alexa-647 dyes per Affimer (see SI). The labeled Affimers were then mixed with a DHLA-ZW-capped CdSe/ZnSe/ZnS QD (λ_{EM} ≈ 606 nm) at different molar ratios but with a fixed total Affimer:QD molar ratio of 12 by adjusting the number of labeled/unlabeled Affimers. This approach was used to minimize the possible change of the QD fluorescence after conjugating with a different number of the His_8-Affimers.[5] As shown in Figure S8 (SI), the QD fluorescence in PBS increased with increasing His_8-Affimer:QD molar ratio initially and became saturated at 12:1, suggesting that 12 copies of Affimer may be assembled onto each QD. The resulting fluorescence spectra was recorded at λ_{EX} = 450 nm, which corresponds to the absorption minimum of the Alexa-647 dye to minimize dye direct excitation. The measurements revealed a progressively quenched QD fluorescence and simultaneously enhanced Alexa-647 FRET signal (~667 nm) with increasing dye/QD ratio, consistent with a QD-sensitized Alex-647 dye FRET mechanism (Figures S9 and S10).[5] The successful QD−Affimer conjugation was also verified by gel electrophoresis, which displayed lower gel mobility than the corresponding non-conjugated QDs (Figure 2F). The QD−Alexa-647 FRET pair has good spectral overlap with a relatively large R_0 value of ~6.5 nm (Figure S9). Using E obtained from QD quenching ($E = 1 - I_{DA}/I_D$, where I_D and I_{DA} are the QD intensity in the absence and presence of the acceptor) and a single QD in FRET interaction with N identical acceptors model ($E = 1/[1 + (r/R_0)^6/N]$),[12] the QD−dye distance r was calculated as ~6.6 ±

DOI: 10.1021/acsami.6b13807
ACS Appl. Mater. Interfaces 2017, 9, 15232−15244

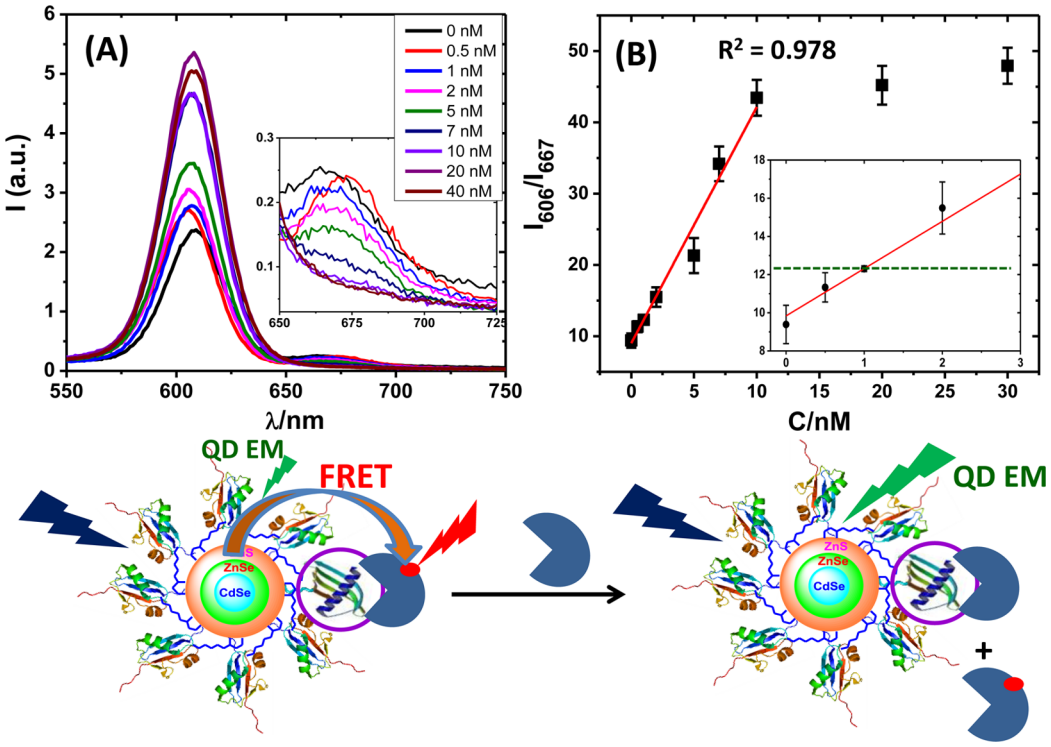

Figure 4. (A) Fluorescence spectra of the QD−Affimer sensor (0.5 nM) after mixing with the Alexa-647-labeled SUMO protein reporter (0.5 nM) containing different amounts of the unlabeled SUMO protein. (B) Plot of I_{606}/I_{667} as a function of the unlabeled SUMO protein concentration: data over 0−10 nM are fitted by a linear function (R^2 = 0.978); inset shows the response over 0−2 nM. Dashed green line shows limit of detection (background +3σ). The scheme below shows the assay principle (the protein circled is the anti-SUMO Affimer, while all others are non-SUMO binding Affimers).

0.5 nm (see SI, Figure S10). This value matched the sum of the Affimer size (~3 nm)[58] and the radius of the CdSe/ZnSe/ZnS QD core ~3.5 nm (Figure S1B) very well. Importantly, a remarkably small r/R_0 value of ~1 was realized with the QD−Affimer conjugate, suggesting it was well suited for FRET-based ratiometric sensing.

We subsequently exploited the use of QD−Affimer to detect the target protein. All sensing experiments were performed in PBS containing a large excess of a nontarget protein (bovine serum albumin, BSA, 1 mg/mL) using a final QD concentration (C_{QD}) of 500 pM unless stated otherwise. The DHLA-ZW ligand-capped CdSe/ZnSe/ZnS QD each conjugated with 12 copies of unlabeled anti-SUMO Affimer (His_8-tagged) was first used to detect the target SUMO protein (Alexa-647 labeled).[58] Figure 3 revealed that with increasing SUMO concentration the QD fluorescence was greatly quenched while the Alexa 647 FRET signal was enhanced simultaneously. This result was fully consistent with a mechanism of QD-sensitized Alexa-647 FRET being induced by the specific Affimer-SUMO binding. The size of acceptor signal enhancement was relatively small in comparison to QD donor quenching, but the results were similar to other QD−Alexa 647 FRET systems reported previously.[14,28] Importantly, the FRET signal of 10 pM SUMO protein was significantly higher than its direct excitation background at 1000-fold higher concentration (10 nM, which was practically the same as the PBS only, see Figure 3A inset), suggesting that the dye direct excitation contribution was negligible. A plot of the integrated fluorescence intensity ratio between the Alexa-647 FRET (from 650 to 750 nm) and the QD (560−650 nm), I_{Dye}/I_{QD}, versus the SUMO concentration yielded a positive linear relationship over 0−500 pM (R^2 = 0.957), suggesting the QD−Affimer sensor can detect pM levels of target protein ratiometrically. Moreover, the linear increase of the I_{Dye}/I_{QD} with the SUMO concentration also matched what was expected from the multiple identical acceptors in FRET interactions with a single QD donor model,[12,29] suggesting that all SUMO proteins were bound to the QD under the same r/R_0 value (see Experimental Section for an explanation).

A distinct advantage of FRET-based sensing over other methods is a ratiometric readout signal with internal self-calibration function. This makes it much less sensitive to instrument noise and/or signal fluctuations, allowing for reliable and accurate target quantitation.[20,29] Moreover, the signal of 10 pM SUMO protein was well separated from the background by >3× standard deviation, 3σ, as indicated by the green dashed line in Figure 3B, inset.[62] This suggests a detection limit of 10 pM for the target SUMO protein, a sensitivity that compares favorably with some other literature QD−FRET sensors for direct protein detection without target amplification (see SI, Table S2). The reasons for the excellent sensitivity here are 2-fold: (1) the UCEP allows the QD to retain a high fluorescence (hence a large R_0); (2) the small size of the Affimer binder leads to a short QD−dye distance r. Both factors are strongly beneficial for improving E and hence sensitivity. Interestingly, the detection limit and linear dynamic range of the QD−Affimer sensor can be readily tuned by the final C_{QD}. Increasing the C_{QD} to 10 nM significantly extended the linear dynamic range to 1−300 nM, although the limit of detection was reduced to ~1 nM (see SI, Figure S11). Moreover, the QD−Affimer sensor specifically detects nM levels of the target SUMO protein even in 50% human serum

DOI: 10.1021/acsami.6b13807
ACS Appl. Mater. Interfaces 2017, 9, 15232−15244

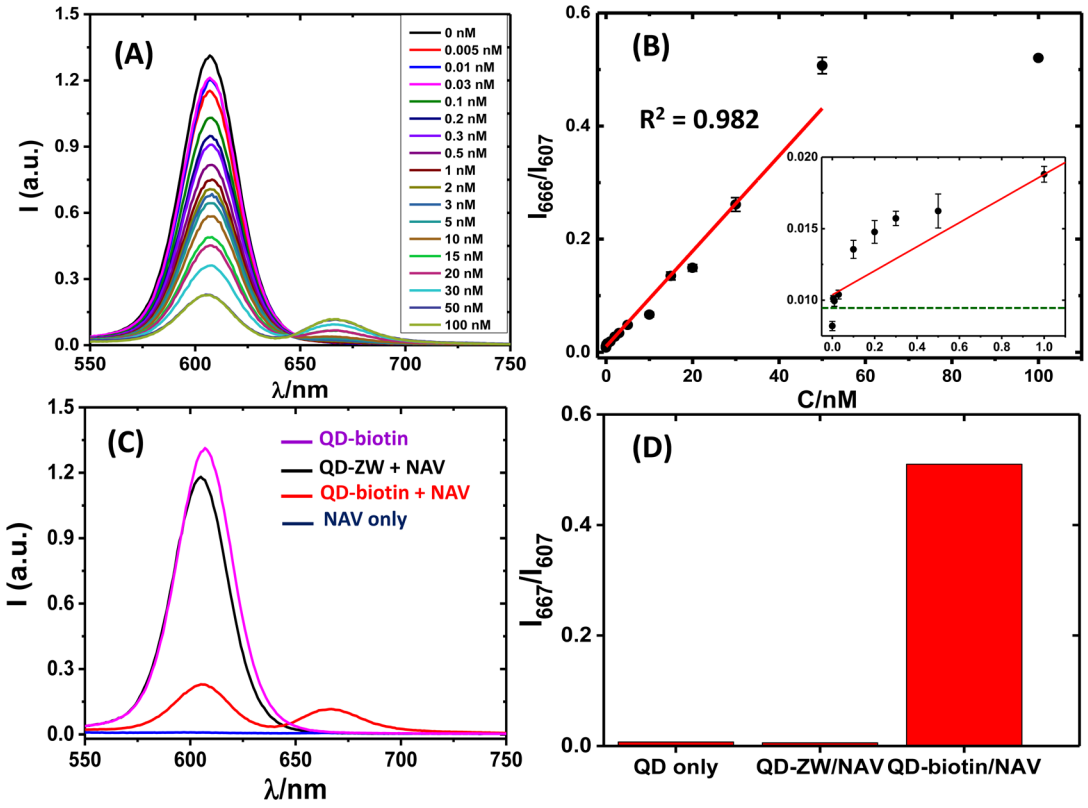

Figure 5. (A) Fluorescence spectra of QD−biotin$_{100}$ (C_{QD} = 0.5 nM) after mixing with different amounts of Alexa-647-labeled neutravidin (NAV). (B) Relationship between the I_{667}/I_{607} and the NAV concentration. Data over 0−50 nM were fitted by a linear function: $Y = 0.01037 + 0.0084X$, R^2 = 0.982 (inset shows the FRET response data over 0−1 nM, and the green dashed line indicates the limit of detection). (C) Fluorescence spectra of 0.5 nM QD−biotin$_{100}$ (purple), 0.5 nM QD−ZW + 50 nM NAV (black), 0.5 nM QD−biotin$_{100}$ + 50 nM NAV (red), and 50 nM NAV only (blue). (D) Comparison of the I_{667}/I_{607} ratios for the QD−biotin$_{100}$ only (QD only), QD−ZW+NAV (QD−ZW/NAV), and QD−biotin$_{100}$+NAV (QD−biotin/NAV). Despite a slight reduction of QD fluorescence of QD−ZW+NAV over QD−biotin$_{100}$ only, their I_{667}/I_{607} ratios were effectively the same, being only ∼1/87 that of the QD−biotin$_{100}$+NAV.

(Figure S12), demonstrating excellent sensing robustness and the potential for clinical applications. This observation is notable as most sensing tests reported were carried out in "clean" buffers, with few demonstrating sensing in clinically relevant solutions,[20,29] especially for the QDs capped with small-molecule ligands.

The ability to detect unlabeled protein target is more useful for biodiagnostics because target labeling may not be feasible for naturally occurring proteins in biological samples. To investigate this potential, we first conjugated each CdSe/ZnSe/ZnS QD with 1 copy of the anti-SUMO Affimer (via His$_8$-tag self-assembly) and then blocked it with 20 copies of a control Affimer (His$_8$-tagged) that showed no affinity to the SUMO protein.[58] An Alexa-647-labeled SUMO protein was then used as a FRET reporter. This design can reduce the chance that an unlabeled SUMO protein will bind to vacant Affimer on the QD surface without displacing a labeled SUMO reporter, thereby improving sensitivity. The final concentrations of the QD and labeled SUMO reporter were fixed at 0.5 nM each. As expected, addition of unlabeled SUMO protein successfully competed with the labeled SUMO bound to the QD−Affimer and generated a sizable QD fluorescence recovery (Figure 4). A plot of the peak intensity ratio between the QD (at 606 nm) and the dye (at 667 nm), I_{606}/I_{667}, versus the unlabeled SUMO concentration revealed a good positive linear relationship over a range of 0−10 nM (R^2 = 0.978) with 1 nM being clearly detected (Figure 4). The label-free sensitivity here was lower than that of labeled detection system (ca. 10 pM). It is likely that multivalency may enhance the Affimer-SUMO binding signal. Moreover, not all of the QD surface target Affimers may be bound to the labeled reporter proteins due to the natural binding−dissociation equilibrium. Thus, some of the introduced unlabeled SUMO proteins may simply bind to the free Affimers on the QD surface without displacing the reporter proteins. Nevertheless, the label-free sensitivity reported here was comparable to most other QD−FRET-based protein sensors (see SI, Table S2).

Preparation of QD−Biotin for Biosensing and Cancer Cell Imaging. Besides preparing stable, biocompatible QDs using nondirectly bioactive DHLA-ligands, the UCEP was further extended to make biotin-functionalized QDs in one pot by treating the CdSe/ZnSe/ZnS QD with DHLA-PEG600-biotin and DHLA-ZW or DHLA-PEG750 spacer ligands (total LQMR = 1000). Tuning the DHLA-PEG600-biotin/spacer ligand molar ratio and treatment sequence allowed for ready control of the QD surface biotin valency. The resulting biotinylated QDs (each having ∼100 DHLA-PEG600-biotin ligands with the rest being DHLA-ZW ligands, denoted as QD−biotin$_{100}$) were employed for the detection of neutravidin (NAV; each labeled with 1.7 Alexa-647 dyes) by exploiting the extremely strong biotin-NAV binding ($K_d \approx 10^{-15}$ M).[63] NAV displays lower nonspecific adsorption than avidin or streptavidin, making it well suited for developing highly specific sensors.[64,65] With increasing amount of NAV added to QD−

DOI: 10.1021/acsami.6b13807
ACS Appl. Mater. Interfaces 2017, 9, 15232−15244

biotin$_{100}$ (C_{QD} = 0.5 nM), the QD fluorescence was progressively quenched while the Alexa-647 FRET signal was enhanced concurrently before reaching saturation at ~50 nM (Figure 5). A control experiment using the QD capped with DHLA-ZW ligands only (QD−ZW, 0.5 nM) after mixing with NAV (50 nM) displayed no detectable FRET signal under identical conditions (Figure 5C and 5D). These results confirm that the FRET signal originates from the specific biotin-NAV binding. A plot of the I_{667}/I_{607} ratio versus NAV concentration gave a good positive linear calibration over the 0−50 nM range (R^2 = 0.982, Figure 5B). Moreover, the signal from 5 pM NAV was well separated from background (by >3σ), suggesting a detection limit of 5 pM. This sensitivity compared favorably against other QD−FRET sensors for protein detection (Table S2). The signal saturation at ≥50 nM NAV suggests that all of the QD surface biotins may have bound to NAV, matching well to the total biotin content expected for 0.5 nM QD−biotin$_{100}$.

Using the labeled NAV as a FRET reporter, the QD−biotin/NAV was further exploited for label-free detection of biotin. Free biotin can compete with QD−biotin$_{100}$ for binding to NAV to reduce the amounts of NAV binding to the QD and hence reduce the FRET signal. Indeed, a significant QD fluorescence recovery together with a concurrently reduced Alex-647 FRET signal was observed as free biotin was added. Moreover, 10 nM biotin was positively detected (SI, Figure S13), suggesting the QD−biotin sensor can be employed for label-free detection of low nM levels of biotin, an example of a small molecule target. The sensitivity here is comparable to a recently reported upconverting nanoparticle-QD FRET sensor for biotin detection (~5 nM).[66]

Biotin is an important vitamin (also known as vitamin H) necessary for cell growth, the production of fatty acids, and the metabolism of fats and amino acids. A number of cancer cells overexpress biotin receptors on their surfaces, making biotin an attractive ligand for cancer targeting.[67−69] Thus, we further investigated the potential of QD−biotin for cancer cell imaging. Two QD samples were prepared with a biotin valency of ~70 and ~150, respectively, with the remaining sites being occupied by DHLA-PEG750 ligands. The QDs, abbreviated as QD−Biotin$_{70}$ and QD−Biotin$_{150}$, respectively, were incubated with the HeLa human cervical cancer cells known to overexpress biotin receptors (see SI for details).[67,69] The resulting confocal fluorescence images revealed that HeLa cells treated with the QD−biotin displayed higher fluorescence intensity than those treated with the DHLA-PEG750 ligand-capped QD control (red channel, Figure 6). This result showed that biotin modification on the QD surface enhanced the uptake by HeLa cells, presumably via biotin receptor-mediated endocytosis. Interestingly, most intracellular QDs appeared to be located close to the cell nuclei (stained by Hoechst and displayed in blue) without entering the nuclei.

A quantitative analysis of individual cell fluorescence intensities at the QD channel by flow cytometry further confirmed that biotin functionalization could enhance cell uptake. Cells incubated with QD−biotin$_{150}$ gave the strongest fluorescence signal, while the control QD exhibited the weakest signal (SI, Figure S14). The median fluorescence intensity of QD−biotin$_{150}$-treated cells was ~56% higher than those treated with the control QD (capped with DHLA-PEG750 ligand only). The level of the cell uptake enhancement observed here was comparable to that reported for other biotinylated nanoparticles.[68] Moreover, cells pretreated with DMEM medium containing 10 mM free biotin for 1 h followed by incubation with QD−biotin$_{150}$ in the presence of 10 mM free biotin resulted in a significantly lower fluorescence intensity (by ~53%) over those pretreated with cell culture medium only followed by incubation with QD−biotin$_{150}$ only (SI, Figure S15). This result revealed that the presence of free biotin reduces the cell uptake of QD−biotin$_{150}$, presumably by competitive binding to cell surface biotin receptors. These results demonstrate a good potential of the biotin-modified QD in targeted cancer cell imaging.

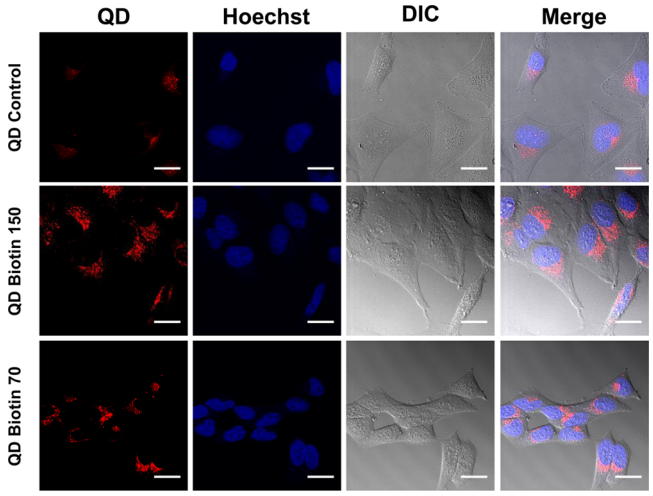

Figure 6. Confocal fluorescence images of HeLa cells after 4 h treatment with 50 nM of the DHLA-PEG750 ligand-capped control QD (top) and two QD−biotin samples containing ~150 (middle) or ~70 (bottom) biotins per QD. From left to right, images are displayed as QD fluorescence image (red), DAPI fluorescence (staining the nuclei, blue), optical image DIC, and the merged fluorescence and optical images.

In summary, an UCEP has been developed that allows for rapid, complete water dispersion of the widely used hydrophobic CdSe/ZnS and CdSe/ZnSe/ZnS QDs using 20−200-fold lower amounts of the DHLA-based ligands over most literature methods. It readily produces compact, biocompatible QDs with excellent stability in biological buffers and retains near native levels of their parent QD fluorescence (>90%). The resulting QD is readily bioconjugated with His$_8$-tagged Affimers for robust, sensitive detection of 10 pM of a specific target protein. It also works robustly in clinically relevant media (50% human serum). The UCEP also allows for simple one-step preparation of biotinylated QDs for sensitive biosensing and targeted cancer cell imaging. Compared to other literature reported QD cap-exchange methods for LA- or DHLA-based ligands, the UCEP has four notable advantages: (1) it uses far fewer ligands (by 20−200-fold), which is extremely valuable for precious, expensive, or difficult to access ligands; (2) it is a rapid procedure; (3) it is easy to operate (using air-stable compounds and rapid in situ reduction under ambient conditions); and (4) it shows no compromise of the fluorescence for the cap-exchanged QDs. Therefore, we believe the UCEP reported herein will impact significantly in the broad QD-based biomedical research field, including biosensing, bioimaging, drug delivery, clinical diagnostics, and therapeutics and most importantly in areas involving the use of QD−FRET-based readout strategies.

DOI: 10.1021/acsami.6b13807
ACS Appl. Mater. Interfaces 2017, 9, 15232−15244

EXPERIMENTAL SECTION

Reagents and Materials. The CdSe/ZnS core/shell QD (λ_{EM} = ~600 nm, quantum yield ≈ 10%) was purchased commercially as dry powders from PlasmaChem GmbH (Berlin, Germany). The QD was capped with mixed ligands of trioctylphosphine oxide (TOPO), hexadecylamine, and oleic acid. Three different colored CdSe/ZnSe/ZnS core/shell/shell QD stocks in toluene (CANdots, λ_{EM}s = ~605, 575, and 525 nm, nominal quantum yield > 30–40%) were purchased from Strem Chemicals UK limited (Cambridge, U.K.). The molar concentrations of the core/shell/shell QD stocks were provided by the supplier. Their extinction coefficients at the first exciton peaks were calculated using the provided stock concentration and their UV–vis absorption spectra. Neutravidin and Hoechst 33342 were purchased from ThermoFisher. Dulbecco's modified Eagle's medium (DMEM), fetal bovine serum (FBS), penicillin, typsin-EDTA, Dulbecco's phosphate buffered saline (PBS), and other chemicals and reagents were all purchased from Sigma-Aldrich (Dorset, UK) and used as received without further purification unless stated otherwise. Solvents were obtained from Fisher Scientific (Loughborough, UK) and used as received. Ultrapure water (resistance > 18.2 MΩ·cm) purified by an ELGA Purelab classic UVF system was used for all experiments and making buffers.[29]

Instruments and Methods. All fluorescence spectra were measured on a Spex Fluoro Max-3 Spectrofluorometer using a 1.5 mL quartz cuvette under a fixed excitation wavelength (λ_{EX}) of 450 nm. This wavelength corresponds to the absorption minimum of the Alexa-647 acceptor, minimizing the FRET background due to direct excitation of the acceptor. An excitation and emission bandwidths of 5 nm and a scan rate of 120 nm/min over 480–800 nm range were used.[29,45] Centrifugations were performed with a Thermo Scientific Heraeus Fresco 21 microcentrifuge. UV–vis absorption spectra were recorded on a Varian Cary 50 Bio UV–visible spectrophotometer over 200–800 nm using a 1 mL quartz cuvette with an optical path of 1 cm or on a Nanodrop 2000 spectrophotometer (Thermo Scientific) over the range of 200–800 nm using 1 drop of the solution with an optical path length of 1 mm. Dynamic light scattering (DLS) was measured using a Zetasizer Nano (Malvern) instrument as described previously.[45] Confocal fluorescence imaging was recorded on a Zeiss LSM-510 inverted laser scanning confocal microscope (Germany) using at 488 nm excitation and collecting emission at above 570 nm.[70] Flow cytometry was recorded on a BD LSRFortessa cytometer. The samples were excited at 488 nm, the emission was collected in the 570–585/42 nm band, and the results were analyzed using the FlowJo v10 software.

Preparation of DHLA-Zwitterion-Capped QDs. The typical ligand exchange procedure for preparing QD–ZW is as follows: commercial hydrophobic CdSe/ZnS or CdSe/ZnSe/ZnS QD (1 nmol, 20 μL in hexane) was precipitated by adding 500 μL of EtOH followed by centrifugation to remove any free TOPO ligands. The QD pellet was dissolved in 50 μL of $CHCl_3$ and then added with 20 μL of EtOH to make solution **A**. LA-ZW (0.10 M, 2 μL in H_2O) was reduced to DHLA-ZW by mixing with TCEP·HCl (0.10 M, 2 μL in H_2O) for 10 min, after which NaOH (0.10 M in EtOH, 12 μL) was added to fully deprotonate the DHLA thiol groups and also to neutralize acid groups in TCEP·HCl (each containing 4 acid groups) to make solution **B**. Solutions **A** and **B** were then mixed in a new Eppendorf tube for 1–3 min with occasional shaking by hand, after which H_2O (50 μL) was added to the reaction mixture. The QD was found to rise to the top aqueous phase, leaving the bottom $CHCl_3$ layer effectively colorless, indicating full QD water solubilization. The top aqueous layer was then carefully separated from the bottom $CHCl_3$ layer and transferred to an Amicon ultracentrifugal tube with a 30 000 MW cutoff membrane and centrifuged for 1 min at 3000 rpm. The residue was washed with H_2O (200 μL) and followed by a brief centrifugation. The process was repeated three times to remove any unbound free ligands, yielding a stable QD aqueous stock solution. The QD concentration was determined by using the corresponding first exciton peak absorbance and extinction coefficient (e.g., 2.6×10^5 $M^{-1}\cdot cm^{-1}$ at ~590 nm for the 600 nm emitting CdSe/ZnS QD, and 4.9×10^5 $M^{-1}\cdot cm^{-1}$ at ~589 nm for the 605 nm emitting CdSe/ZnSe/ZnS QD) using the Beer–Lambert Law following our previously established procedures.[29,30,45]

Protein Labeling. The yeast SUMO protein target and the anti-SUMO Affimer were expressed in BL21 (DE3) cells using isopropyl β-D-1-thiogalactopyranoside (IPTG) induction and purified by Ni-NTA resin (Qiagen) affinity chromatography following the manufacturer's instructions. The detailed experimental procedures were described in our recent publication.[58] The anti-SUMO Affimer (5 mg/mL, 12.5 μL in PBS, MW = 13 267) in a microcentrifuge tube was first mixed with Alexa 647 NHS-ester (50 μg in 2 μL DMSO), and then 5 μL of $NaHCO_3$ (0.5 M, pH = 8.3) and 7.5 μL of PBS (10 mM phosphate, 150 mM NaCl, pH 7.4) were added and thoroughly mixed at room temperature for 2 h (dye:protein molar ratio ≈ 8:1). The reaction mixture was loaded onto a G25 gel fitration column using PBS for elution by gravity flow. The first eluted blue band (corresponding to the labeled anti-SUMO Affimer) was collected, and its absorption spectrum was recorded. Using the extinction coefficients of the Alexa-647 dye ($\varepsilon_{650\ nm}$ = 239 000 $M^{-1}\cdot cm^{-1}$) and Affimer ($\varepsilon_{280\ nm}$ = 7904 $M^{-1}\cdot cm^{-1}$) and the $CF_{280\ nm}$ of 0.03 for the Alexa-647 dye, the average dye labeling ratio on per Affimer was calculated as 1.08 with a stock protein concentration of 86 μM.[45] Similarly, the SUMO protein was labeled with Alexa-647 NHS ester under a dye:protein molar ratio of 6.4 and yielded an average dye per protein label ratio of 0.80. Neutravidin was also labeled with Alexa-647 NHS ester under a dye:protein molar ratio of 7, giving an average Alexa-647 dye label per protein of 1.67.

QD–Affimer Biosensing. All sensing experiments were performed in PBS containing 1 mg/mL of bovine serum albumin (BSA, to minimize the nonspecific adsorption of the QD/proteins on surfaces) at a final QD concentration (C_{QD}) of 0.50 nM at a volume of 800 μL unless otherwise stated. For labeled detection, the DHLA-ZW-capped QD (QD–ZW) was first mixed with the unlabeled anti-SUMO Affimer (His_8-tagged) at a protein:QD molar ratio of 12 in a quartz cuvette and incubated for 20 min. Then varying amounts of target SUMO protein (Alexa-647 labeled) were added and incubated for another 15 min before the fluorescence spectra were recorded. For label-free detection, the QD–ZW was first incubated with 1 mol equiv of the anti-SUMO Affimer for 10 min and then blocked with 20 mol equiv of a control Affimer for 20 min. Then QD molar equivalent of the Alexa-647-labeled SUMO protein (used as the FRET reporter) mixed with varying amounts of the unlabeled SUMO protein was then introduced and incubated for a further 20 min before the fluorescence spectra were recorded.

QD–Biotin Biosensing. The assay procedures were similar to the QD–Affimer sensing above. The biotin-functionalized QDs (each having ~100 DHLA-PEG600-biotin with the rest being DHLA-ZW ligands, denoted as QD–$biotin_{100}$) were mixed with different amounts of the Alexa-647-labeled neutravidin (NAV) and incubated for 20 min before fluorescence spectra were recorded. For biotin detection, Alexa-647-labeled Neutravidin (50 nM) was mixed with different amounts of free biotin for 20 min before being added to the QD–$biotin_{100}$ (C_{QD} = 0.5 nM). After a further 20 min incubation, the resulting fluorescence spectra were recorded.

Gel Electrophoresis. A 2 or 5 μL amount of a DHLA-ZW-capped CdSe/ZnS core/shell QD (QD–ZW, λ_{EM} ≈ 600 nm) prepared at a LQMR of 200, 500, and 1000 was mixed with 18 or 15 μL of 60% glycerol in H_2O. A QD–Affimer assembly was also prepared by mixing the QD–ZW prepared at a LQMR of 500 with 10 mol equiv of the His_8-tagged Affimer. The resulting QD–Affimer conjugate was treated in the same manner as the QD–ZW samples. Then 20 μL of each sample was loaded onto a 0.75% agarose gel in TAE buffer pH 8.3. Samples were separated at 100 mV for ~30 min, and QDs were visualized under UV illumination (λ = 365 nm).

Cell Culture. HeLa-adherent epithelial cells derived from human cervical carcinoma were grown in Dulbecco's modified Eagle's medium (DMEM) supplemented with 10% (v/v) fetal bovine serum (FBS) and 100 U mL^{-1} penicillin. The HeLa cells were trypsinized using trypsin-EDTA and maintained in a humidified incubator with 5% CO_2 at 37 °C.

DOI: 10.1021/acsami.6b13807
ACS Appl. Mater. Interfaces 2017, 9, 15232–15244

Laser Scanning Confocal Microscopy. A 2 mL amount of HeLa cells (1.5×10^5 cells mL^{-1}) was cultured for 24 h followed by treatment with 1 mL of the serum-free DMEM with or without the QD samples (50 nM). After incubation for 4 h, the cells were washed three times with Dulbecco's phosphate-buffered saline. Hoechst 33342 was added to a final concentration of 5 μg mL^{-1} for nuclei staining. The cells were then imaged by laser scanning confocal microscopy (Zeiss LSM-510 inverted laser scanning confocal microscope, Germany). The QD was excited at 488 nm and the emission above 570 nm was collected.

Flow Cytometry. A 1 mL amount of HeLa cells (3×10^5 cells/mL) was cultured in 6-well plates for 24 h followed by treatment with 1 mL of serum-free DMEM with or without QDs (50 nm). After 4 h incubation, the cells were washed three times with Dulbecco's phosphate-buffered saline (D-PBS). After cell detachment using 0.5 mL of trypsin-EDTA, 0.5 mL of serum-free DMEM was added to each well and the samples were centrifuged in 2 mL microcentrifuge tubes for 5 min at 1000 rpm. The supernatant was discarded and replaced with 0.5 mL of serum-free DMEM. The samples were filtered using Flowmi cell strainers (40 μm) and analyzed in 5 mL Falcon plastic tubes using a BD LSRFortessa cytometer. The samples were excited at 488 nm, and the emission was collected in the 570−585/42 nm band. The results were analyzed using FlowJo v10 software.

Free Biotin Competition. A 1 mL amount of HeLa cells (3×10^5 cells/mL) was cultured in 6-well plates for 24 h, followed by 1 h treatment of one set of triplicates with 10 mM free biotin in serum-free DMEM. A 1 mL amount of serum-free DMEM with QD (50 nM) with or without free biotin (10 mM) was then added to the wells which had been pretreated with free biotin or incubated normally, respectively. After a 4 h incubation, the cells were washed three times with PBS. After cell detachment using 0.5 mL of Trypsin-EDTA, 0.5 mL of serum-free DMEM was added to each well and the samples were centrifuged in 2 mL microcentrifuge tubes for 5 min at 1000 rpm. The supernatant was discarded and replaced with 0.5 mL of serum-free DMEM. The samples were filtered using Flowmi cell strainers (40 μm) and analyzed in 5 mL Falcon plastic tubes using BD LSRFortessa cytometer. The samples were excited at 488 nm, and the emission was collected in the 586/16 nm band. The results were analyzed using FlowJo v10 software.

Correlation between the FRET Ratio and QD-Bound Protein. For a single QD donor in FRET interaction with N identical acceptors (e.g., idential QD−dye distance, r), the FRET efficiency, E, is given in the following equation[12]

$$E = N \times R_0^6/(N \times R_0^6 + r^6) = 1/[1 + (r/R_0)^6/N] \quad (1)$$

where R_0 is the Förster radius of the QD−single dye FRET pair and r is donor−acceptor distance. E can be measured from the enhanced acceptor emission by

$$E = I_{Dye}/[I_{Dye} + \beta I_{QD}] = 1/[1 + \beta I_{QD}/I_{Dye}] \quad (2)$$

where β is a correction factor for the different donor/acceptor quantum yield and detection efficiency. Assuming the shape of the QD and dye fluorescence spectra are independent of intensity then the integrated I_{QD}/I_{Dye} ratio should be linearly propotional to the peak intensity ratio, e.g., $I_{QD}/I_{Dye} = \alpha I_{606}/I_{667}$ (α is a correction factor between the integrated and the peak intensity ratio). Combination of eqs 1 and 2 gives

$$1/[1 + I_{QD}/I_{Dye}] = 1/[1 + \alpha\beta \times I_{606}/I_{667}] = 1/[1 + (r/R_0)^6/N] \quad (3)$$

This yields the following relationship

$$I_{QD}/I_{Dye} = \alpha\beta \times I_{606}/I_{667} = (r/R_0)^6/N \quad (4)$$

Hence

$$I_{QD}/I_{Dye} = N \times [(R_0/r)^6] \quad (5)$$

$$I_{667}/I_{606} = N \times [\alpha\beta \times (R_0/r)^6] \quad (6)$$

This reveals that both the FRET ratio, I_{Dye}/I_{QD}, and the apparent FRET ratio, I_{667}/I_{606}, should increase linearly with N, the number of acceptors (proteins) bound to the QD under the same FRET distance (or r/R_0 ratio).

■ ASSOCIATED CONTENT

Supporting Information

The Supporting Information is available free of charge on the ACS Publications website at DOI: 10.1021/acsami.6b13807.

Experimental details which include the synthesis and characterization of three lipoic acid-based ligands; supporting figures showing the QD size, calculations of the Zn^{2+} ion footprint, QD−Alexa 647 Förster radius (R_0), and average FRET distance (r) of the QD−Affimer conjugate; target protein detection in serum and extending sensing dynamic range; label-free biotin detection and flow cytometry results showing biotin modification enhancing the QD uptake and free biotin competing this uptake; supporting tables showing the QD hydrodynamic size and sensing performance comparison (PDF)

■ AUTHOR INFORMATION

Corresponding Author

*E-mail: d.zhou@leeds.ac.uk. Tel: +44-113-3436230. Fax: +44-113-3436565.

ORCID

Rongjun Chen: 0000-0002-8133-5472

Dejian Zhou: 0000-0003-3314-9242

Author Contributions

D.Z. conceived the research and supervised the experiments; W.W., Y.G., C.T., S.C., M.K., Y.K., and A.K. performed the research; W.W., M.K., R.C., and D.Z. analyzed the data; D.Z. wrote the paper. All authors have read, commented, and approved the final version of the paper.

Notes

The authors declare the following competing financial interest(s): The University of Leeds has filed a patent application on the Adhiron technology on which M.J.M. and D.C.T. are identified as inventors (PCT/GB-2014/050435). Adhiron binders are marketed commercially as Affimers by Avacta Life Sciences (U.K.).

■ ACKNOWLEDGMENTS

We thank Dr. Mike Ward (University of Leeds) for help in TEM imaging. We also thank the University of Leeds, the Leeds Biomedical Health Research Centre, Imperial College London, and the Wellcome Trust for funding this work. Y.G. thanks the Wellcome Trust (UK, Grant No. 097354/Z/11/Z) for providing a Career Re-entry fellowship. S.C. thanks Imperial College London for providing a fully funded Ph.D. Scholarship. M.K. thanks the Biotechnology and Biological Sciences Research Council (BBSRC, Grant No. BB/L016044/1) and MedImmune for awarding an Industrial CASE Ph.D. Studentship.

■ REFERENCES

(1) Bruchez, M., Jr.; Moronne, M.; Gin, P.; Weiss, S.; Alivisatos, A. P. Semiconductor Nanocrystals as Fluorescent Biological Labels. *Science* **1998**, *281*, 2013−2016.

DOI: 10.1021/acsami.6b13807
ACS Appl. Mater. Interfaces 2017, 9, 15232−15244

(2) Chan, W. C. W.; Nie, S. M. Quantum Dot Bioconjugates for Ultrasensitive Nonisotopic Detection. *Science* **1998**, *281*, 2016−2018.
(3) Medintz, I. L.; Mattoussi, H. Quantum Dot-based Resonance Energy Transfer and Its Growing Application in Biology. *Phys. Chem. Chem. Phys.* **2009**, *11*, 17−45.
(4) Larson, D. R.; Zipfel, W. R.; Williams, R. M.; Clark, S. W.; Bruchez, M. P.; Wise, F. W.; Webb, W. W. Water-soluble Quantum Dots for Multiphoton Fluorescence Imaging in Vivo. *Science* **2003**, *300*, 1434−1436.
(5) Medintz, I. L.; Clapp, A. R.; Mattoussi, H.; Goldman, E. R.; Fisher, B.; Mauro, J. M. Self-assembled Nanoscale Biosensors based on Quantum Dot FRET Donors. *Nat. Mater.* **2003**, *2*, 630−638.
(6) Michalet, X.; Pinaud, F. F.; Bentolila, L. A.; Tsay, J. M.; Doose, S.; Li, J. J.; Sundaresan, G.; Wu, A. M.; Gambhir, S. S.; Weiss, S. Quantum Dots for Live Cells, in Vivo Imaging, and Diagnostics. *Science* **2005**, *307*, 538−544.
(7) Wegner, K. D.; Hildebrandt, N. Quantum dots: Bright and Versatile in Vitro and in Vivo Fluorescence Imaging Biosensors. *Chem. Soc. Rev.* **2015**, *44*, 4792−4834.
(8) Somers, R. C.; Bawendi, M. G.; Nocera, D. G. CdSe Nanocrystal based Chem-/bio-sensors. *Chem. Soc. Rev.* **2007**, *36*, 579−591.
(9) Hildebrandt, N.; Spillmann, C. M.; Algar, W. R.; Pons, T.; Stewart, M. H.; Oh, E.; Susumu, K.; Díaz, S. A.; Delehanty, J. B.; Medintz, I. L. Energy Transfer with Semiconductor Quantum Dot Bioconjugates: A Versatile Platform for Biosensing, Energy Harvesting, and Other Developing Applications. *Chem. Rev.* **2017**, *117*, 536−711.
(10) Zhou, D. J.; Bruckbauer, A.; Abell, C.; Klenerman, D.; Kang, D. J. Fabrication of Three-dimensional Surface Structures with Highly Fluorescent Quantum Dots by Surface-templated Layer-by-layer Assembly. *Adv. Mater.* **2005**, *17*, 1243−1248.
(11) Tikhomirov, G.; Hoogland, S.; Lee, P. E.; Fischer, A.; Sargent, E. H.; Kelley, S. O. DNA-Based Programming of Quantum Dot Valency, Self-Assembly and Luminescence. *Nat. Nanotechnol.* **2011**, *6*, 485−490.
(12) Clapp, A. R.; Medintz, I. L.; Mauro, J. M.; Fisher, B. R.; Bawendi, M. G.; Mattoussi, H. Fluorescence Resonance Energy Transfer between Quantum Dot Donors and Dye-labeled Protein Acceptors. *J. Am. Chem. Soc.* **2004**, *126*, 301−310.
(13) Medintz, I. L.; Konnert, J. H.; Clapp, A. R.; Stanish, I.; Twigg, M. E.; Mattoussi, H.; Mauro, J. M.; Deschamps, J. R. A Fluorescence Resonance Energy Transfer-Derived Structure of A Quantum Dot-Protein Bioconjugate Nanoassembly. *Proc. Natl. Acad. Sci. U. S. A.* **2004**, *101*, 9612−9617.
(14) Chang, E.; Miller, J. S.; Sun, J. T.; Yu, W. W.; Colvin, V. L.; Drezek, R.; West, J. L. Protease-Activated Quantum Dot Probes. *Biochem. Biophys. Res. Commun.* **2005**, *334*, 1317−1321.
(15) Goldman, E. R.; Medintz, I. L.; Whitley, J. L.; Hayhurst, A.; Clapp, A. R.; Uyeda, H. T.; Deschamps, J. R.; Lassman, M. E.; Mattoussi, H. A Hybrid Quantum Dot-antibody Fragment Fluorescence Resonance Energy Transfer-based TNT Sensor. *J. Am. Chem. Soc.* **2005**, *127*, 6744−6751.
(16) Dubertret, B.; Skourides, P.; Norris, D. J.; Noireaux, V.; Brivanlou, A. H.; Libchaber, A. In Vivo Imaging of Quantum Dots Encapsulated in Phospholipid Micelles. *Science* **2002**, *298*, 1759−1762.
(17) Zhang, C. Y.; Yeh, H. C.; Kuroki, M. T.; Wang, T. H. Single-Quantum-Dot-Based DNA Nanosensor. *Nat. Mater.* **2005**, *4*, 826−831.
(18) Zhang, H.; Zhou, D. A Quantum Dot-Intercalating Dye Dual-Donor FRET Based Biosensor. *Chem. Commun.* **2012**, *48*, 5097−5099.
(19) Zhou, D. Quantum Dot-Nucleic Acid/Aptamer Bioconjugate-based Fluorimetric Biosensors. *Biochem. Soc. Trans.* **2012**, *40*, 635−639.
(20) Wegner, K. D.; Jin, Z.; Linden, S.; Jennings, T. L.; Hildebrandt, N. Quantum-Dot-Based Forster Resonance Energy Transfer Immunoassay for Sensitive Clinical Diagnostics of Low-Volume Serum Samples. *ACS Nano* **2013**, *7*, 7411−7419.
(21) Yu, W. W.; Chang, E.; Falkner, J. C.; Zhang, J. Y.; Al-Somali, A. M.; Sayes, C. M.; Johns, J.; Drezek, R.; Colvin, V. L. Forming Biocompatible and Nonaggregated Nanocrystals in Water Using Amphiphilic Polymers. *J. Am. Chem. Soc.* **2007**, *129*, 2871−2879.
(22) Howarth, M.; Liu, W.; Puthenveetil, S.; Zheng, Y.; Marshall, L. F.; Schmidt, M. M.; Wittrup, K. D.; Bawendi, M. G.; Ting, A. Y. Monovalent, Reduced-Size Quantum Dots for Imaging Receptors on Living Cells. *Nat. Methods* **2008**, *5*, 397−399.
(23) Mattoussi, H.; Palui, G.; Na, H. B. Luminescent Quantum Dots as Platforms for Probing in Vitro and in Vivo Biological Processes. *Adv. Drug Delivery Rev.* **2012**, *64*, 138−166.
(24) Algar, W. R.; Kim, H.; Medintz, I. L.; Hildebrandt, N. Emerging Non-Traditional Förster Resonance Energy Transfer Configurations with Semiconductor Quantum Dots: Investigations and Applications. *Coord. Chem. Rev.* **2014**, *263-264*, 65−85.
(25) Zhou, D. J.; Piper, J. D.; Abell, C.; Klenerman, D.; Kang, D. J.; Ying, L. M. Fluorescence Resonance Energy Transfer Between a Quantum Dot Donor and A Dye Acceptor Attached to DNA. *Chem. Commun.* **2005**, 4807−4809.
(26) Clapp, A. R.; Medintz, I. L.; Mattoussi, H. Forster Resonance Energy Transfer Investigations Using Quantum-Dot Fluorophores. *ChemPhysChem* **2006**, *7*, 47−57.
(27) Pons, T.; Medintz, I. L.; Wang, X.; English, D. S.; Mattoussi, H. Solution-Phase Single Quantum Dot Fluorescence Resonance Energy Transfer. *J. Am. Chem. Soc.* **2006**, *128*, 15324−15331.
(28) Zhou, D.; Li, Y.; Hall, E. A. H.; Abell, C.; Klenerman, D. A Chelating Dendritic Ligand Capped Quantum Dot: Preparation, Surface Passivation, Bioconjugation and Specific DNA Detection. *Nanoscale* **2011**, *3*, 201−211.
(29) Zhang, H.; Feng, G.; Guo, Y.; Zhou, D. Robust and Specific Ratiometric Biosensing Using A Copper-Free Clicked Quantum Dot-DNA Aptamer Sensor. *Nanoscale* **2013**, *5*, 10307−10315.
(30) Zhou, D.; Ying, L.; Hong, X.; Hall, E. A.; Abell, C.; Klenerman, D. A Compact Functional Quantum Dot-DNA Conjugate: Preparation, Hybridization, and Specific Label-free DNA Detection. *Langmuir* **2008**, *24*, 1659−1664.
(31) Pong, B. K.; Trout, B. L.; Lee, J. Y. Modified Ligand-exchange for Efficient Solubilization of CdSe/ZnS Quantum Dots in Water: A Procedure Guided by Computational Studies. *Langmuir* **2008**, *24*, 5270−5276.
(32) Algar, W. R.; Krull, U. J. Luminescence and Stability of Aqueous Thioalkyl Acid Capped CdSe/ZnS Quantum Dots Correlated to Ligand Ionization. *ChemPhysChem* **2007**, *8*, 561−568.
(33) Susumu, K.; Uyeda, H. T.; Medintz, I. L.; Pons, T.; Delehanty, J. B.; Mattoussi, H. Enhancing the Stability and Biological Functionalities of Quantum Dots via Compact Multifunctional Ligands. *J. Am. Chem. Soc.* **2007**, *129*, 13987−13996.
(34) Liu, W.; Howarth, M.; Greytak, A. B.; Zheng, Y.; Nocera, D. G.; Ting, A. Y.; Bawendi, M. G. Compact Biocompatible Quantum Dots Functionalized for Cellular Imaging. *J. Am. Chem. Soc.* **2008**, *130*, 1274−1284.
(35) Muro, E.; Pons, T.; Lequeux, N.; Fragola, A.; Sanson, N.; Lenkei, Z.; Dubertret, B. Small and Stable Sulfobetaine Zwitterionic Quantum Dots for Functional Live-Cell Imaging. *J. Am. Chem. Soc.* **2010**, *132*, 4556−4557.
(36) Susumu, K.; Mei, B. C.; Mattoussi, H. Multifunctional Ligands Based on Dihydrolipoic Acid and Polyethylene Glycol to Promote Biocompatibility of Quantum Dots. *Nat. Protoc.* **2009**, *4*, 424−436.
(37) Zhan, N. Q.; Palui, G.; Safi, M.; Ji, X.; Mattoussi, H. Multidentate Zwitterionic Ligands Provide Compact and Highly Biocompatible Quantum Dots. *J. Am. Chem. Soc.* **2013**, *135*, 13786−13795.
(38) Zhan, N. Q.; Palui, G.; Kapur, A.; Palomo, V.; Dawson, P. E.; Mattoussi, H. Controlling the Architecture, Coordination, and Reactivity of Nanoparticle Coating Utilizing an Amino Acid Central Scaffold. *J. Am. Chem. Soc.* **2015**, *137*, 16084−16097.
(39) Ma, L.; Tu, C. L.; Le, P.; Chitoor, S.; Lim, S. J.; Zahid, M. U.; Teng, K. W.; Ge, P. H.; Selvin, P. R.; Smith, A. M. Multidentate Polymer Coatings for Compact and Homogeneous Quantum Dots with Efficient Bioconjugation. *J. Am. Chem. Soc.* **2016**, *138*, 3382−3394.

DOI: 10.1021/acsami.6b13807
ACS Appl. Mater. Interfaces 2017, 9, 15232−15244

(40) Liu, W. H.; Greytak, A. B.; Lee, J.; Wong, C. R.; Park, J.; Marshall, L. F.; Jiang, W.; Curtin, P. N.; Ting, A. Y.; Nocera, D. G.; Fukumura, D.; Jain, R. K.; Bawendi, M. G. Compact Biocompatible Quantum Dots via RAFT-Mediated Synthesis of Imidazole-Based Random Copolymer Ligand. *J. Am. Chem. Soc.* **2010**, *132*, 472−483.
(41) Wang, W.; Ji, X.; Kapur, A.; Zhang, C.; Mattoussi, H. A Multifunctional Polymer Combining the Imidazole and Zwitterion Motifs as a Biocompatible Compact Coating for Quantum Dots. *J. Am. Chem. Soc.* **2015**, *137*, 14158−14172.
(42) Zhan, N.; Palui, G.; Merkl, J.-P.; Mattoussi, H. Bio-orthogonal Coupling as a Means of Quantifying the Ligand Density on Hydrophilic Quantum Dots. *J. Am. Chem. Soc.* **2016**, *138*, 3190−3201.
(43) Jeong, S.; Achermann, M.; Nanda, J.; Ivanov, S.; Klimov, V. I.; Hollingsworth, J. A. Effect of the Thiol-thiolate Equilibrium on the Photophysical Properties of Aqueous CdSe/ZnS Nanocrystal Quantum Dots. *J. Am. Chem. Soc.* **2005**, *127*, 10126−10127.
(44) Liu, D.; Snee, P. T. Water-Soluble Semiconductor Nanocrystals Cap Exchanged with Metalated Ligands. *ACS Nano* **2011**, *5*, 546−550.
(45) Guo, Y.; Sakonsinsiri, C.; Nehlmeier, I.; Fascione, M. A.; Zhang, H.; Wang, W.; Poehlmann, S.; Turnbull, W. B.; Zhou, D. Compact, Polyvalent Mannose Quantum Dots as Sensitive, Ratiometric FRET Probes for Multivalent Protein-Ligand Interactions. *Angew. Chem., Int. Ed.* **2016**, *55*, 4738−4742.
(46) Aldeek, F.; Hawkins, D.; Palomo, V.; Safi, M.; Palui, G.; Dawson, P. E.; Alabugin, I.; Mattoussi, H. UV and Sunlight Driven Photoligation of Quantum Dots: Understanding the Photochemical Transformation of the Ligands. *J. Am. Chem. Soc.* **2015**, *137*, 2704−2714.
(47) Palui, G.; Avellini, T.; Zhan, N. Q.; Pan, F.; Gray, D.; Alabugin, I.; Mattoussi, H. Photoinduced Phase Transfer of Luminescent Quantum Dots to Polar and Aqueous Media. *J. Am. Chem. Soc.* **2012**, *134*, 16370−16378.
(48) Zhan, N. Q.; Palui, G.; Grise, H.; Tang, H. L.; Alabugin, I.; Mattoussi, H. Combining Ligand Design with Photoligation to Provide Compact, Colloidally Stable, and Easy to Conjugate Quantum Dots. *ACS Appl. Mater. Interfaces* **2013**, *5*, 2861−2869.
(49) Zhan, N.; Palui, G.; Mattoussi, H. Preparation of Compact Biocompatible Quantum Dots Using Multicoordinating Molecular-scale Ligands Based on A Zwitterionic Hydrophilic Motif and Lipoic Acid Anchors. *Nat. Protoc.* **2015**, *10*, 859−874.
(50) Tamang, S.; Beaune, G.; Texier, I.; Reiss, P. Aqueous Phase Transfer of InP/ZnS Nanocrystals Conserving Fluorescence and High Colloidal Stability. *ACS Nano* **2011**, *5*, 9392−9402.
(51) Dai, M. Q.; Yung, L. Y. L. Ethylenediamine-Assisted Ligand Exchange and Phase Transfer of Oleophilic Quantum Dots: Stripping of Original Ligands and Preservation of Photoluminescence. *Chem. Mater.* **2013**, *25*, 2193−2201.
(52) Greytak, A. B.; Allen, P. M.; Liu, W. H.; Zhao, J.; Young, E. R.; Popovic, Z.; Walker, B. J.; Nocera, D. G.; Bawendi, M. G. Alternating Layer Addition Approach to CdSe/CdS Core/Shell Quantum Dots with Near-Unity Quantum Yield and High On-Time Fractions. *Chem. Sci.* **2012**, *3*, 2028−2034.
(53) Susumu, K.; Oh, E.; Delehanty, J. B.; Blanco-Canosa, J. B.; Johnson, B. J.; Jain, V.; Hervey, W. J.; Algar, W. R.; Boeneman, K.; Dawson, P. E.; Medintz, I. L. Multifunctional Compact Zwitterionic Ligands for Preparing Robust Biocompatible Semiconductor Quantum Dots and Gold Nanoparticles. *J. Am. Chem. Soc.* **2011**, *133*, 9480−9496.
(54) Chen, Y.; Vela, J.; Htoon, H.; Casson, J. L.; Werder, D. J.; Bussian, D. A.; Klimov, V. I.; Hollingsworth, J. A. "Giant" Multishell CdSe Nanocrystal Quantum Dots with Suppressed Blinking. *J. Am. Chem. Soc.* **2008**, *130*, 5026−5027.
(55) Kim, S.; Fisher, B.; Eisler, H. J.; Bawendi, M. Type-II Quantum Dots: CdTe/CdSe(Core/Shell) and CdSe/ZinTe(Core/Shell) Heterostructures. *J. Am. Chem. Soc.* **2003**, *125*, 11466−11467.
(56) Mattera, L.; Bhuckory, S.; Wegner, K. D.; Qiu, X.; Agnese, F.; Lincheneau, C.; Senden, T.; Djurado, D.; Charbonniere, L. J.; Hildebrandt, N.; Reiss, P. Compact Quantum Dot-antibody Conjugates for FRET Immunoassays with Subnanomolar Detection Limits. *Nanoscale* **2016**, *8*, 11275−11283.
(57) Wegner, K. D.; Linden, S.; Jin, Z. W.; Jennings, T. L.; el Khoulati, R.; Henegouwen, P.; Hildebrandt, N. Nanobodies and Nanocrystals: Highly Sensitive Quantum Dot-Based Homogeneous FRET Immunoassay for Serum-Based EGFR Detection. *Small* **2014**, *10*, 734−740.
(58) Tiede, C.; Tang, A. A. S.; Deacon, S. E.; Mandal, U.; Nettleship, J. E.; Owen, R. L.; George, S. E.; Harrison, D. J.; Owens, R. J.; Tomlinson, D. C.; McPherson, M. J. Adhiron: A Stable and Versatile Peptide Display Scaffold for Molecular Recognition Applications. *Protein Eng., Des. Sel.* **2014**, *27*, 145−155.
(59) Fisher, M. J.; Williamson, D. J.; Burslem, G. M.; Plante, J. P.; Manfield, I. W.; Tiede, C.; Ault, J. R.; Stockley, P. G.; Plein, S.; Maqbool, A.; Tomlinson, D. C.; Foster, R.; Warriner, S. L.; Bon, R. S. Trivalent Gd-DOTA Reagents for Modification of Proteins. *RSC Adv.* **2015**, *5*, 96194−96200.
(60) Raina, M.; Sharma, R.; Deacon, S. E.; Tiede, C.; Tomlinson, D.; Davies, A. G.; McPherson, M. J.; Walti, C. Antibody Mimetic Receptor Proteins for Label-free Biosensors. *Analyst* **2015**, *140*, 803−810.
(61) Zhang, Y.; Zhang, H.; Hollins, J.; Webb, M. E.; Zhou, D. Small-molecule Ligands Strongly Affect the Forster Resonance Energy Transfer Between a Quantum Dot and a Fluorescent Protein. *Phys. Chem. Chem. Phys.* **2011**, *13*, 19427−19436.
(62) Rissin, D. M.; Kan, C. W.; Campbell, T. G.; Howes, S. C.; Fournier, D. R.; Song, L.; Piech, T.; Patel, P. P.; Chang, L.; Rivnak, A. J.; Ferrell, E. P.; Randall, J. D.; Provuncher, G. K.; Walt, D. R.; Duffy, D. C. Single-molecule Enzyme-linked Immunosorbent Assay Detects Serum Proteins at Subfemtomolar Concentrations. *Nat. Biotechnol.* **2010**, *28*, 595−599.
(63) Thermo Scientific Pierce Protein Research Products 2009 Catalog; https://thermofisher.portica.de/system/includes/download.php?f=1033.
(64) Zhang, Y.; Pilapong, C.; Guo, Y.; Ling, Z. L.; Cespedes, O.; Quirke, P.; Zhou, D. J. Sensitive, Simultaneous Quantitation of Two Unlabeled DNA Targets Using a Magnetic Nanoparticle-Enzyme Sandwich Assay. *Anal. Chem.* **2013**, *85*, 9238−9244.
(65) Zhang, Y.; Guo, Y.; Quirke, P.; Zhou, D. J. Ultrasensitive Single-nucleotide Polymorphism Detection Using Target-recycled Ligation, Strand Displacement and Enzymatic Amplification. *Nanoscale* **2013**, *5*, 5027−5035.
(66) Mattsson, L.; Wegner, K. D.; Hildebrandt, N.; Soukka, T. Upconverting Nanoparticle to Quantum Dot FRET for Homogeneous Double-nano Biosensors. *RSC Adv.* **2015**, *5*, 13270−13277.
(67) Park, S.; Kim, E.; Kim, W. Y.; Kang, C.; Kim, J. S. Biotin-guided Anticancer Drug Delivery with Acidity-Triggered Drug Release. *Chem. Commun.* **2015**, *51*, 9343−9345.
(68) Wang, J.; Wang, F.; Li, F.; Zhang, W.; Shen, Y.; Zhou, D.; Guo, S. A Multifunctional Poly(curcumin) Nanomedicine for Dual-modal Targeted Delivery, Intracellular Responsive Release, Dual-drug Treatment and Imaging of Multidrug Resistant Cancer Cells. *J. Mater. Chem. B* **2016**, *4*, 2954−2962.
(69) Lv, L.; Guo, Y.; Shen, Y.; Liu, J.; Zhang, W.; Zhou, D.; Guo, S. Intracellularly Degradable, Self-Assembled Amphiphilic Block Copolycurcumin Nanoparticles for Efficient In Vivo Cancer Chemotherapy. *Adv. Healthcare Mater.* **2015**, *4*, 1496−1501.
(70) Zhang, W.; Wang, F.; Wang, Y.; Wang, J.; Yu, Y.; Guo, S.; Chen, R.; Zhou, D. pH and Near-infrared Light Dual-stimuli Responsive Drug Delivery Using DNA-conjugated Gold Nanorods for Effective Treatment of Multidrug Resistant Cancer Cells. *J. Controlled Release* **2016**, *232*, 9−19.

DOI: 10.1021/acsami.6b13807
ACS Appl. Mater. Interfaces 2017, 9, 15232−15244